Available online at www.sciencedirect.com
ScienceDirect
Trans. Nonferrous Met. Soc. China 33(2023) 209−219
Transactions of Nonferrous Metals Society of China
www.tnmsc.cn

Domain knowledge aided machine learning method for properties prediction of soft magnetic metallic glasses

Xin LI[1,2], Guang-cun SHAN[1,2], Hong-bin ZHAO[3], Chan Hung SHEK[2]

1. School of Instrumentation Science and Opto-electronics Engineering, Beihang University, Beijing 100191, China;
2. Department of Materials Science and Engineering,
City University of Hong Kong, Kowloon Tong, Hong Kong SAR, China;
3. State Key Laboratory of Advanced Materials for Smart Sensing, GRINM Group Co., Ltd., Beijing 100088, China

Received 30 September 2021; accepted 24 February 2022

Abstract: A machine learning (ML) method aided by domain knowledge was proposed to predict saturated magnetization (B_s) and critical diameter (D_{max}) of soft magnetic metallic glasses (MGs). Two datasets were established based on published experimental works about soft magnetic MGs. A general feature space was proposed and proven to be adaptive for ML model training for different prediction tasks. It was demonstrated that the predictive performance of ML models was better than that of traditional knowledge-based estimation methods. In addition, domain knowledge aided feature design can greatly reduce the number of features without significantly reducing the prediction accuracy. Finally, the binary classification of D_{max} of soft magnetic MGs was studied.

Key words: metallic glass; soft magnetism; glass forming ability; machine learning; material descriptor

1 Introduction

Soft magnetic metallic glasses (MGs) have attracted considerable attention due to their unique combination of excellent mechanical and magnetic properties [1]. Due to the amorphous structure, soft magnetic MGs usually do not have magnetic anisotropy and grain boundaries, which make them exhibit excellent soft magnetic properties, i.e., high permeability and saturated magnetization (B_s) and low coercivity. For the functional engineering application of soft magnetic MGs, the main goal is to improve B_s. B_s is an intrinsic property of magnetic materials, which refers to the maximum flux density that can be achieved. In general, MGs with high B_s value have a high content of ferromagnetic elements, for example, 1.75 T for $Fe_{86}B_7C_7$ ribbon [2], 1.82 T for $(Fe_{0.8}Co_{0.2})_{87}B_7Si_3P_3$ ribbon [3], 1.9 T for $(Fe_{0.8}Co_{0.2})_{85}B_{14}Si_1$ ribbon [4], 1.51 T for $Fe_{76}Si_9B_{10}P_5$ rod with a critical diameter (D_{max}) of 2.5 mm [5], and 1.61 T for $Fe_{75.3}C_7Si_{3.3}B_5P_{8.7}Cu_{0.7}$ rod with a D_{max} of 1.5 mm [6]. D_{max} is the diameter of the largest amorphous rod that an alloying composition can form. It is an experimental parameter that could be easily obtained and is often used to quantify glass forming ability (GFA) of MGs. Though ~5000 MG compositions have been developed [7], most of them were in a ribbon form and showed too limited GFA to form bulk MGs with large geometric size. Therefore, understanding B_s and D_{max} of soft magnetic MGs is an important research topic, and prediction of the two properties is of great significance for the design of high performance soft magnetic MGs.

In the past few years, machine learning (ML) has been applied to material science to predict the

Corresponding author: Guang-cun SHAN, Tel: +86-10-82339603, E-mail: gcshan@buaa.edu.cn;
Chan Hung SHEK, E-mail: apchshek@cityu.edu.hk
DOI: 10.1016/S1003-6326(22)66101-6

material properties or behaviors [8−10]. GFA and magnetic properties of alloys also have been studied by ML methods, which can be divided into classification and regression. For classification, ML models based on backpropagation neural network [11], support vector machine [12], general and transferable deep learning framework [13], etc., were trained to identify MGs and non-MGs classes. For regression analysis, ML models were trained to predict the specific D_{max} value of MGs [14,15] and the B_s value of MGs [16] and nanocrystalline alloys [17].

In this work, a ML method aided by domain knowledge was proposed to predict B_s and D_{max} of soft magnetic MGs based on alloying compositions. Two datasets were established based on previous work. ML models were trained based on five ML algorithms, and their predictive performance was compared. A general feature space was proposed for the prediction of the two properties, and feature design based on domain knowledge was conducted. By comparing the predictive performance of ML models before and after feature selection, the effect of domain knowledge in the ML method was highlighted.

2 Methodology

2.1 Dataset description

The two datasets were deduced from previous work. A data entry in the datasets contains information about the chemical compositions and the experimental values of target properties, i.e., B_s and D_{max}. The saturated magnetization dataset (hereinafter referred to as BS Dataset) contains 639 alloying compositions, most of them were taken from a previous related work [18], and the rest were collected from other published literature [19−23]. Since the mean magnetic moment of iron is larger than that of cobalt and nickel, and the cost of production of the former is lower than the latter, Fe-based MGs become the mainstream in soft magnetic MGs. The critical casting diameter dataset (hereinafter referred to as DMAX Dataset) contains 519 alloying compositions, which were selected from two previous related works [14,24]. The literature [24] provided a Fe-based bulk MGs dataset containing 480 alloying compositions with experimental D_{max} values. Another literature [14] provided a bulk MGs dataset containing 7950 alloying compositions with experimental D_{max} values, out of which 139 are Fe-based bulk MGs. The D_{max} values of the same alloying composition reported in different works may be different, and in this case, the average value was adopted.

Figures 1(a, b) show the value distribution of B_s and D_{max}, respectively. The value of B_s in the dataset ranges from 0.05 to 1.92 T with a median of 1.5 T and an average of 1.19 T, which shows the excellent magnetic property of MGs. The value of D_{max} in the dataset ranges from 0.06 to 18.00 mm with a median of 2.50 mm and an average of 3.04 mm. The D_{max} data are sparsely distributed in the interval greater than 7 mm, which indicates that improving GFA of MGs is still challenging. Figures 1(c, d) show the distribution of chemical elements in the two datasets. There are 33 and 29 kinds of chemical elements in BS Dataset and DMAX Dataset, respectively, and ~95% of the alloying compositions contain Fe and B. As mentioned before, Fe is the main ferromagnetic element used in soft magnetic MGs. Proper addition of boron could enhance GFA of Fe-based MGs without excessively negative effect on the magnetic properties [25]. Figures 1(c, d) also indicate that a lot of chemical elements could be used for the preparation of soft magnetic MGs. Therefore, an effective properties prediction method is of great significance for the development of new soft magnetic MGs.

In general, soft magnetic alloys can be easily magnetized and demagnetized, which is usually identified by whether the values of their intrinsic coercivity (H_c) are less than 1 kA/m. A scatter plot of the values of B_s versus H_c of the alloying compositions in BS Dataset is shown in Fig. 2(a), which indicates that they exhibit typical soft magnetic property. Most of the alloying compositions have a H_c value even lower than 50 A/m. There are 130 alloying compositions with both B_s and D_{max} values. As shown in Fig. 2(b), B_s and D_{max} values of these alloying compositions show a weak negative correlation. Their Pearson correlation coefficient was calculated to be −0.10, which confirms the negative correlation. The calculation method of Pearson correlation coefficient could be found in the previous work [18]. Therefore, in general, B_s and D_{max} values of Fe-based MGs are

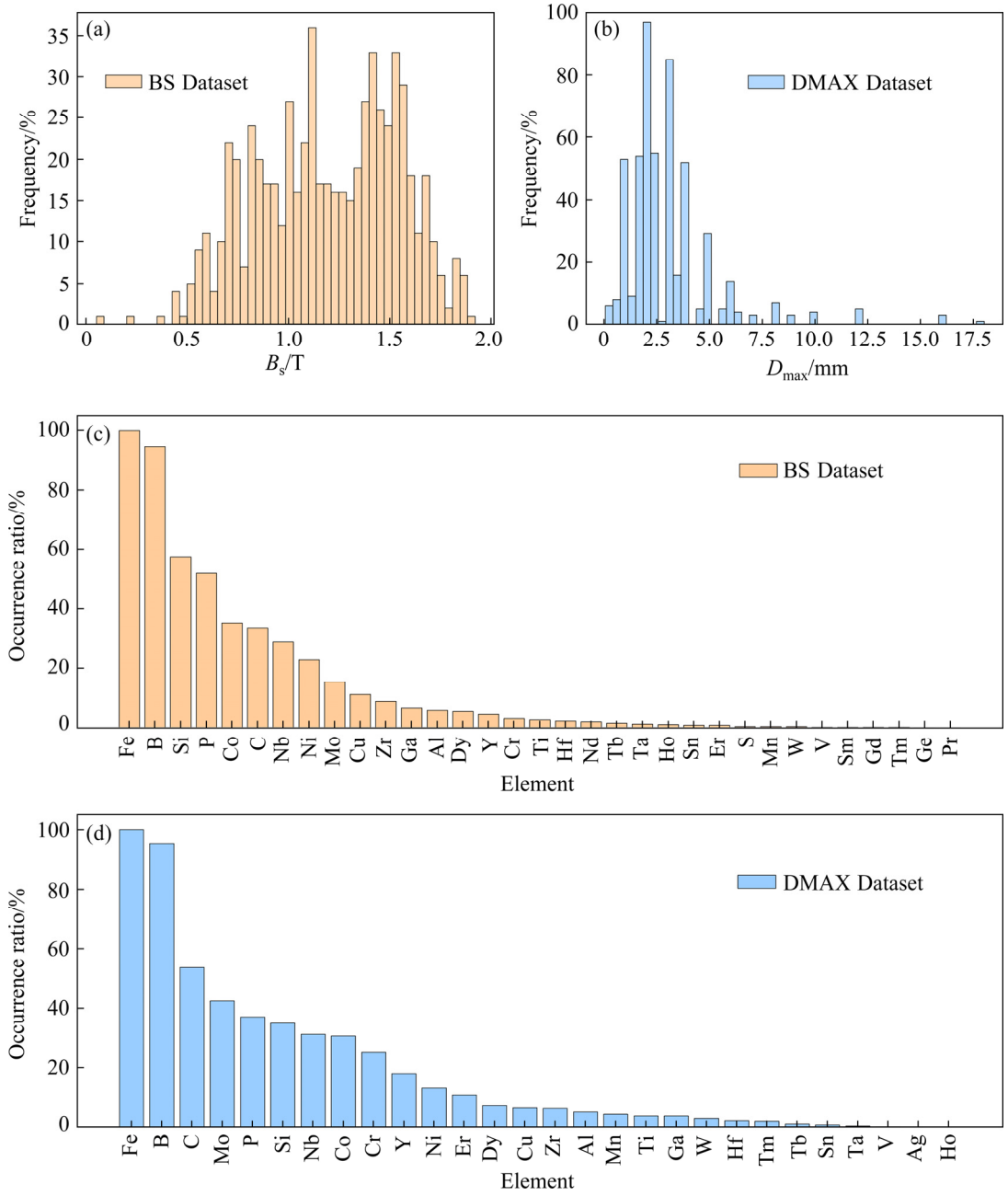

Fig. 1 Distribution of B_s (a), D_{max} (b), and chemical elements in BS Dataset (c) and DMAX Dataset (d)

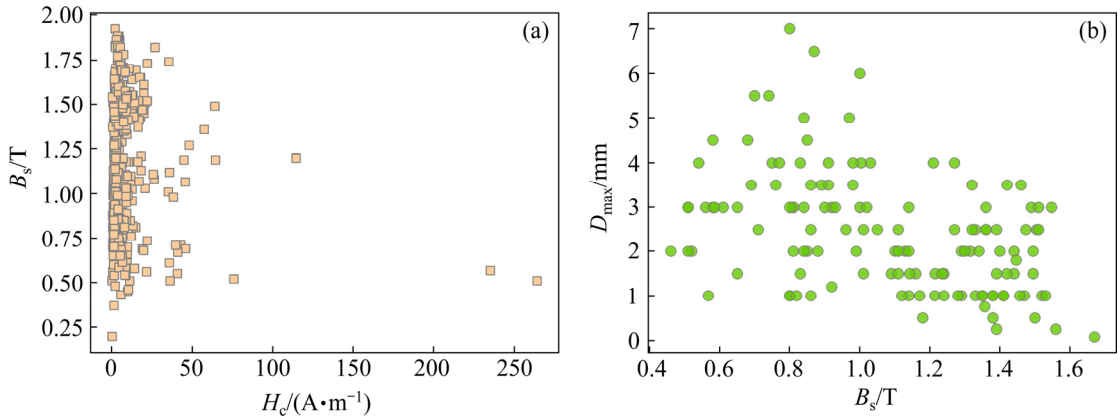

Fig. 2 Scatter plots of B_s versus H_c (a) and D_{max} versus B_s (b)

incompatible with each other to some extent. Understanding and modeling the two properties could help to design high performance soft magnetic MGs.

2.2 General feature space

Feature space is a combination of some measurable parameters used to describe the input, which is alloying composition in this work, of ML models. For designing new functional alloys with desired properties, it is more practical not to involve any parameters about synthesis process or experimental measurements. Therefore, the features used in this work to describe soft magnetic MGs compositions were all only based on chemical compositions and elemental properties. A general feature space was proposed to conduct ML model training and prediction of both B_s and D_{max}. Apart from the feature candidates used in the previous work [18], including elements and molar fraction (c), theoretical density (ρ), mean metallic atomic radius [26] (R_m), atomic size difference (δ_R), theoretical molar volume [27] (V_m), melting temperature calculated by the rule of mixtures (T_m), Pauling electronegativity [26] (χ), valence electron concentration [28] (VEC) and mixing entropy [29] (ΔS_{mix}), more feature candidates were involved in this work, including mixing enthalpy [30] (ΔH_{mix}), mixing Gibbs free energy [14] (ΔG_{mix}), Pauling electronegativity difference (δ_χ), relative Pauling electronegativity (R_χ), valence electron concentration difference (δ_{VEC}), relative valence electron concentration (RVEC), work function [31] (W) and work function difference (δ_W), as given in Table 1. All the feature candidates in the general feature space can be divided into four classes related to chemical components, atomic structures, thermo-dynamics and electronic properties. The feature candidates related to atomic structures, thermodynamics and electronic properties mainly describe the molar fraction weighted average and mismatch of the elemental properties in alloying compositions by

$$\overline{r} = \sum_{i=1}^{n} c_i p_i \tag{1}$$

$$\delta = \sqrt{\sum_{i=1}^{n} c_i \left(1 - \frac{p_i}{\overline{p}}\right)^2} \tag{2}$$

where n is the total number of chemical elements in an alloying composition, and c_i and p_i are the molar fraction and elemental properties of the i-th element, respectively. In addition, ΔS_{mix}, ΔH_{mix}, ΔG_{mix}, R_χ and RVEC are calculated by

$$\Delta S_{mix} = -R\sum_{i=1}^{n} c_i \ln c_i \tag{3}$$

$$\Delta H_{mix} = \sum_{i=1}^{n} 4 c_i c_j \Delta H_{AB}^{mix},\ i \neq j \tag{4}$$

$$\Delta G_{mix} = \Delta H_{mix} - T_m \Delta S_{mix} \tag{5}$$

$$R_\chi = \sum_{i=1}^{n} c_i \chi_i - c_{Fe}\chi_{Fe} - c_{Co}\chi_{Co} - c_{Ni}\chi_{Ni} - c_{Gd}\chi_{Gd} \tag{6}$$

$$\mathrm{RVEC} = \sum_{i=1}^{n} c_i \mathrm{VEC}_i - c_{Fe}\mathrm{VEC}_{Fe} - c_{Co}\mathrm{VEC}_{Co} - c_{Ni}\mathrm{VEC}_{Ni} - c_{Gd}\mathrm{VEC}_{Gd} \tag{7}$$

where χ_i and VEC_i are the electronegativity and valence electron concentration of the i-th element, respectively, and c_j is the molar fraction of the j-th element. R is the molar gas constant, and ΔH_{AB}^{mix} is the mixing enthalpy of the liquid binary alloy containing the i-th and the j-th elements. χ_{Fe}=1.83, χ_{Co}=1.88, χ_{Ni}=1.91, χ_{Gd}=1.2, VEC_{Fe}=8, VEC_{Co}=9,

Table 1 General feature space used for ML model training and prediction

Feature class	Description
Chemical composition	Molar fraction of chemical elements (c)
Related to atomic structures	Theoretical density (ρ)
	Mean metallic atomic radius (R_m)
	Atomic size difference (δ_R)
	Theoretical molar volume (V_m)
Related to thermodynamics	Mixing entropy (ΔS_{mix})
	Mixing enthalpy (ΔH_{mix})
	Mixing Gibbs free energy (ΔG_{mix})
	Melting temperature calculated by rule of mixtures (T_m)
Related to electronic properties	Pauling electronegativity (χ)
	Pauling electronegativity difference (δ_χ)
	Relative Pauling electronegativity (R_χ)
	Valence electron concentration (VEC)
	Valence electron concentration difference (δ_{VEC})
	Relative valence electron concentration (RVEC)
	Work function (W)
	Work function difference (δ_W)

VEC_{Ni}=10 and VEC_{Gd}=3.

2.3 Knowledge-based feature design

The general feature space contained as much information as possible to be applicable to different prediction tasks. Although the theoretically calculated features have contained domain knowledge, too many features might hide the physical mechanism dominating the target properties, and redundant information also had a negative impact on the predictive performance of ML models. Therefore, feature selection was conducted. First, several prevalent feature selection methods from machine learning community were used to reduce the number of features for B_s and D_{max} prediction without significant loss of accuracy. Then, a knowledge-based feature was added to improve the predictive performance of ML models. In the first feature selection process, three feature selection algorithms were used, namely univariate feature selection [32], feature importance given by light gradient boosting machine (LightGBM) [33] and recursive feature elimination (RFE) [34], which were denoted as M1, M2 and M3, respectively. Univariate feature selection can figure out the features having the strongest relationship with the target variable by statistical tests. The statistical test used in this work is the analysis of variance with the F-test [32]. LightGBM is a decision tree-based algorithm, which could produce feature importance by traversing each node of the established trees with a criterion. RFE recursively removes unimportant features suggested by ML models and trains a new ML model using the remaining features in the feature list. The ML algorithm used for producing feature importance in RFE is also LightGBM. The first feature selection procedure is mainly based on the principle of statistical analysis, which is data-sensitive. In addition, many researchers have studied magnetic properties and GFA of MGs from a material science point of view, which can be used to guide feature design. For example, according to the theories in magnetism, B_s is proportional to the mean magnetic moment of all the atoms in an alloy [35], which is described by

$$B_s = \frac{N_A \bar{\mu} \mu_B}{V_m} \tag{8}$$

where N_A is Avogadro constant, $\bar{\mu}$ is the mean magnetic moment of the alloy, and μ_B is Bohr magneton. Furthermore, since the 1930s, some theoretical estimation methods for the mean magnetic moment of an alloy have been continuously developed [36]. Recently, based on free electron transfer theory, an estimation method of $\bar{\mu}$ was proposed for Fe-based alloys using the chemical compositions [35]. Inspired by that work, the estimated $\bar{\mu}$ is selected as a feature.

2.4 Machine learning algorithms

Kinds of ML algorithms have been successfully applied to solving material science problems, but there is no universal ML algorithm. Therefore, it is necessary to choose a suitable ML algorithm and implement hyperparameters optimization for good predictive performance in different problems. Five ML algorithms were selected to address the problem of B_s and D_{max} prediction in this work, namely support vector regression (SVR) [37], multilayer perceptron (MLP) [37], random forest (RF) [38], extreme gradient boosting (XGBoost) [39] and LightGBM. Their predictive performance was evaluated by 10-fold cross-validation [40], which is a prevalent method to objectively evaluate the predictive performance of ML models when the dataset size is limited. The evaluation metric used in cross-validation was root mean squared error (RMSE) calculated by

$$\mathrm{RMSE}(y_i, \hat{y}_i) = \sqrt{\frac{1}{n}\sum_{i=1}^{n}(y_i - \hat{y}_i)^2} \tag{9}$$

where y_i is the experimental value of B_s or D_{max}, and $\hat{y}_i$ is the predicted value of y_i. The unit of RMSE is the same as the target variable, and the smaller the RMSE value, the better the predictive performance of the ML model. The final predictive performance was quantified by the average value of ten RMSE scores produced by 10-fold cross-validation, and the ML algorithm with the lowest RMSE value was suggested as the most suitable algorithm for B_s or D_{max} prediction. In addition, to compare the prediction accuracy of the two target properties (B_s and D_{max}) with different unit, another metric, namely determination coefficient (R^2), was calculated by

$$R^2(y_i, \hat{y}_i) = 1 - \sum_{i=0}^{n}(y_i - \hat{y}_i)^2 \Big/ \sum_{i=0}^{n}(y_i - \bar{y})^2 \tag{10}$$

where $\bar{y}$ is the average value of y_i.

3 Results and discussion

3.1 ML models trained with general feature space

Based on the general feature space, the predictive performance of the five ML algorithms was evaluated via 10-fold cross-validation. The cross-validation results evaluated by RMSE and R^2 are shown in Fig. 3. It was found that XGBoost model outperformed others with the lowest RMSE and highest R^2 for both B_s and D_{max} prediction. Figure 3(b) showed that the prediction accuracy for D_{max} was much lower than that for B_s. The reason could be that D_{max} Dataset is scattered, and the data density is too large for the range of under 5 mm, which indicates that GFA of most reported MGs is limited. In addition, the experimental D_{max} of MGs is measured by the injection casting method. The cooling rate of rods in copper mold casting is hard to keep uniform in different experiments. Therefore, the experimentally measured D_{max} values could be fluctuated. The R^2 values of B_s and D_{max} prediction via XGBoost were ~0.93 and ~0.68, respectively, which were consistent with the recently reported results in MGs [16,18,24,41]. It should be noted that all the ML models were trained based on the same feature space, i.e., the general feature space mentioned above.

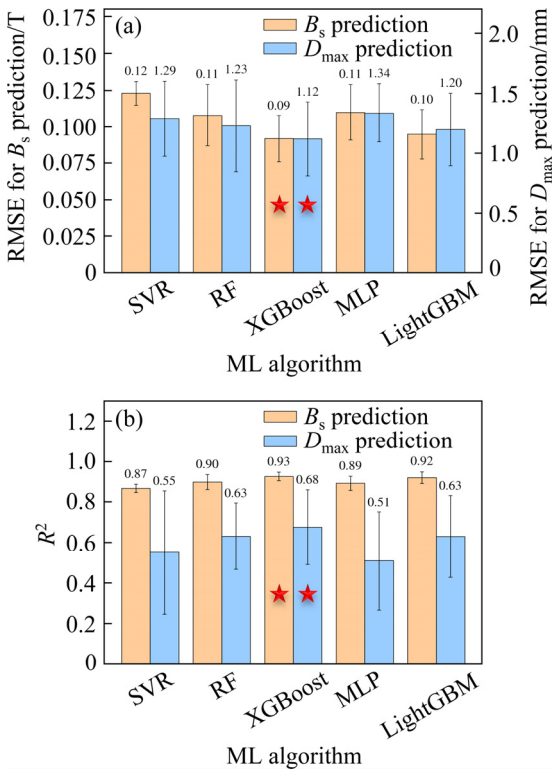

Fig. 3 Cross-validation evaluated by RMSE (a) and R^2 (b) of different ML algorithms

3.2 ML models trained with selected feature space

Based on the general feature space, feature selection was conducted. In the first feature selection procedure, every feature selection strategy (M1, M2 and M3) was set to recommend 15 features out of the general feature space. Then, ten features were finally selected based on the recommendations. The feature selection results for B_s and D_{max} prediction are listed in Table 2. It should be noted that the finally selected ten features were not presented in any order of priority.

Table 2 Feature selection for prediction of B_s and D_{max} in soft magnetic MGs

Target	Method	Recommended feature
B_s	M1	ΔG_{mix}, R_χ, RVEC, ΔS_{mix}, c_{Fe}, δ_{VEC}, c_{Nb}, δ_R, c_{Ni}, ΔH_{mix}, c_B, c_{Dy}, c_{Co}, T_m, ρ
	M2	T_m, ρ, χ, ΔG_{mix}, ΔH_{mix}, VEC, δ_{VEC}, W, R_m, ΔS_{mix}, V_m, δ_χ, RVEC, R_χ, c_{Fe}
	M3	c_{Fe}, ρ, δ_R, R_χ, δ_{VEC}, RVEC, ΔS_{mix}, T_m, ΔH_{mix}, ΔG_{mix}, VEC, δ_χ, R_m, V_m, χ
	Final	c_{Fe}, ρ, δ_R, R_χ, δ_{VEC}, RVEC, ΔS_{mix}, T_m, ΔH_{mix}, ΔG_{mix}
D_{max}	M1	ΔG_{mix}, R_χ, RVEC, δ_χ, ΔS_{mix}, c_{Cr}, T_m, VEC, c_{Mo}, δ_R, c_{Tm}, ρ, c_C, ΔH_{mix}, c_P
	M2	RVEC, T_m, ΔH_{mix}, ΔG_{mix}, δ_χ, ΔS_{mix}, χ, R_m, R_χ, VEC, ρ, δ_{VEC}, δ_R, W, c_{Fe}
	M3	ρ, R_m, δ_R, χ, δ_χ, R_χ, VEC, δ_{VEC}, RVEC, V_m, ΔS_{mix}, T_m, ΔH_{mix}, ΔG_{mix}, W
	Final	ρ, δ_R, χ, δ_χ, R_χ, RVEC, ΔS_{mix}, T_m, ΔH_{mix}, ΔG_{mix}

Since XGBoost showed the best predictive performance in the general feature space, the impact of feature selection on its predictive performance was evaluated by cross-validation using the same hyperparameters as before. Figure 4 shows the scatter plots of all the cross-validated predictions for B_s and D_{max}. By comparing Figures 4(a, b), it can be found that the accuracy of B_s prediction was slightly decreased after feature selection. Based on the final 10 features selected for B_s prediction in Table 2, the estimated $\bar{\mu}$ [35] of each alloying compositions in BS Dataset was calculated and

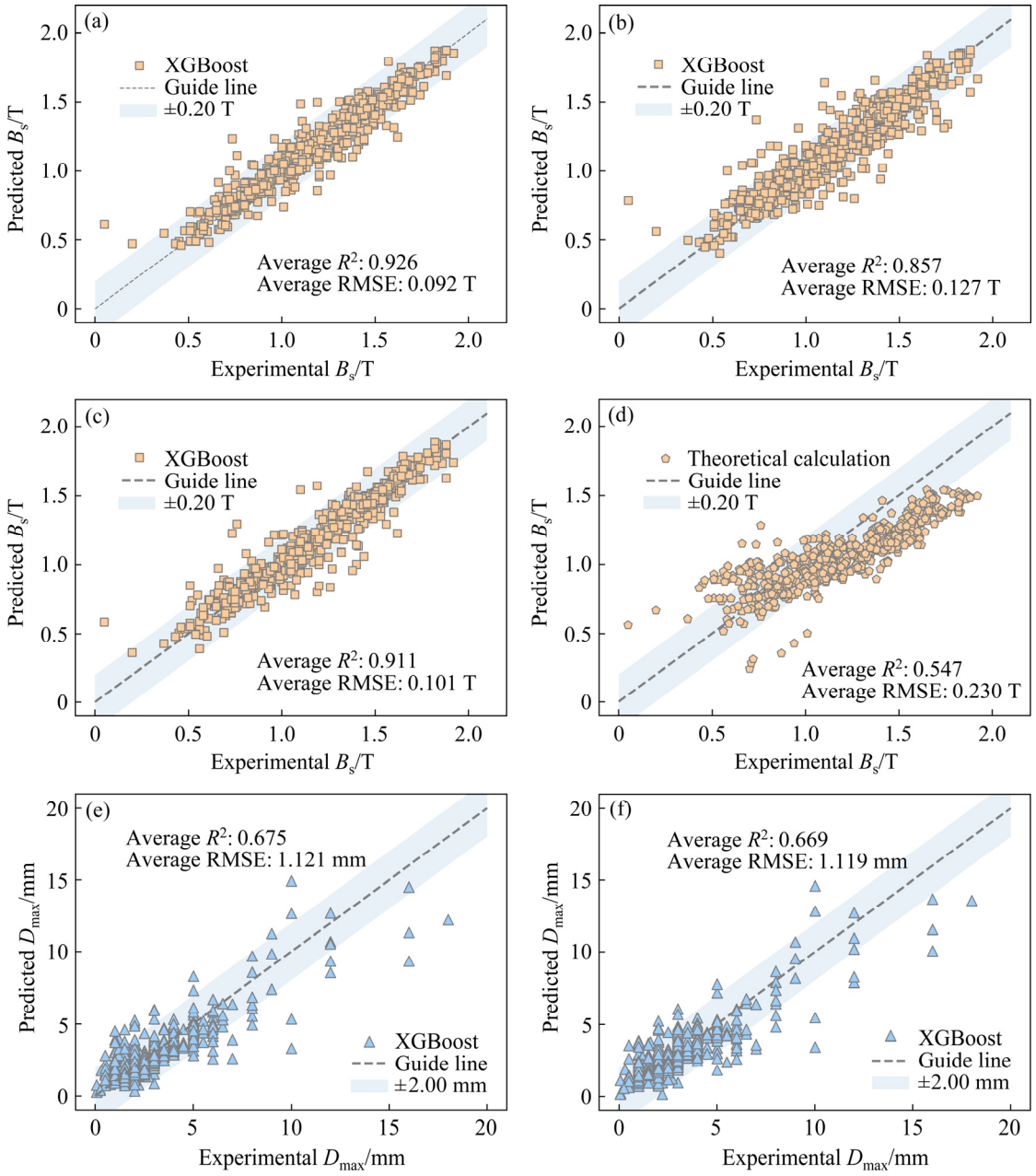

Fig. 4 Cross-validated predictions of B_s based on general feature space (a), selected 10 features (b), selected 11 features with $\bar{\mu}$ (c) and theoretical calculation (d), and D_{max} based on general feature space (e) and selected 10 features (f)

added as a feature. As shown in Fig. 4(c), after adding this feature, the accuracy of B_s prediction was improved a lot with R^2 increasing from 0.857 to 0.911, and RMSE decreasing from 0.127 to 0.101 T. Therefore, the estimated $\bar{\mu}$ made a positive contribution to the predictive performance of XGBoost model. However, if B_s was calculated directly by Eq. (8) based on the estimated $\bar{\mu}$, the accuracy would be much lower than that of XGBoost model. As shown in Fig. 4(d), R^2 and RMSE values for this theoretical calculation method are only 0.547 and 0.230 T, respectively. The $\bar{\mu}$ estimation method for MGs was developed from free electron transfer theory, which is of great significance for understanding the magnetic properties of MGs. However, to accurately predict magnetic properties of MGs, more factors should be considered. According to the feature selection results, apart from features about electron transfer (R_χ, δ_{VEC} and RVEC), other features about structures (c_{Fe}, ρ and δ_R) and thermodynamic properties (ΔS_{mix}, T_m, ΔH_{mix} and ΔG_{mix}) also had an impact on the prediction accuracy of B_s.

For D_{max} prediction, the prediction accuracy

just slightly decreased after feature selection, as shown in Figs. 4(e, f). The R^2 slightly decreased from 0.675 to 0.669, and RMSE slightly decreased from 1.121 to 1.119 mm. However, the number of features was greatly reduced from 44 to 10. A large reduction in the number of features is very helpful in improving the robustness of ML models and reduce the complexity of ML models. Though the prediction accuracy of D_{max} via ML models was not as satisfactory as B_s, it had outperformed any traditional GFA descriptors based on experimental thermal dynamic parameters [41], for example, onset crystallization temperature (T_x), glass transition temperature (T_g), liquidus temperature (T_l) and supercooled liquid region (ΔT_x). In addition, the ML-based GFA prediction method does not rely on any experimental parameter, which has more practical value in discovering new MGs.

More details in 10-fold cross-validation are shown in Fig. 5. The same 10-fold dataset splitting was used for ML model training based on different feature spaces. In general, the sub-fold fluctuation of RMSE or R^2 had a similar tendency for different feature spaces. A ML model with a smaller sub-fold fluctuation means that its predictive performance is more robust. From this point, feature selection had little impact on the robustness of the ML models for B_s or D_{max} prediction.

3.3 D_{max} classification

Since D_{max} distribution in the dataset is too unbalanced to achieve regression analysis with high accuracy, classification analysis was conducted. A binary classification task was presented by setting the critical D_{max} to be 3 mm, which means that the whole dataset was divided into two parts, i.e., positive samples (D_{max}>3 mm) and negative samples (D_{max}<3 mm). The five ML algorithms used in previous regression were also suitable for classification. It should be noted that the corresponding classification algorithm of SVR is named support vector classifier (SVC) [37]. They are different implementations of support vector machines. The classification performance of different ML models was also compared by the 10-fold cross-validation strategy. As shown in Fig. 6(a), the classification performance of the five ML algorithms was comparable, and RF reached

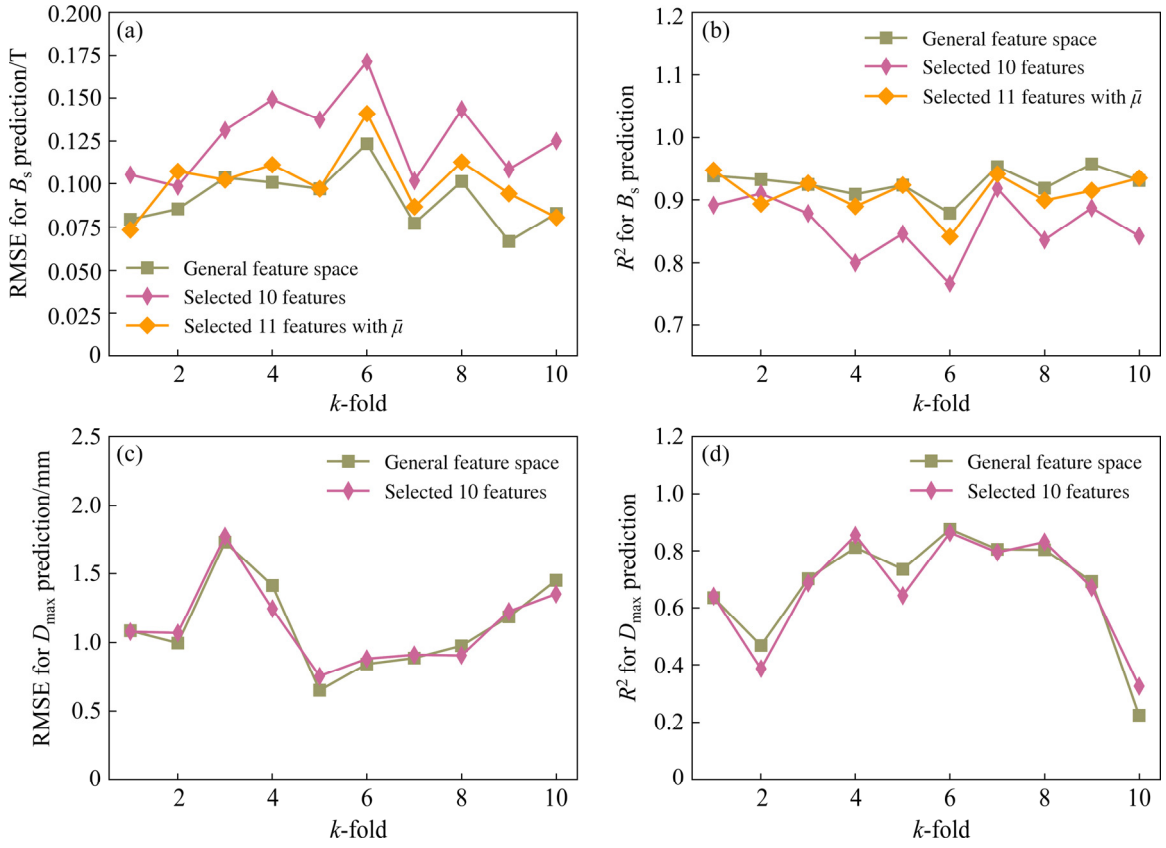

Fig. 5 Detailed scores in 10-fold cross-validation: (a, b) RMSE and R^2 for B_s prediction; (c, d) RMSE and R^2 for D_{max} prediction

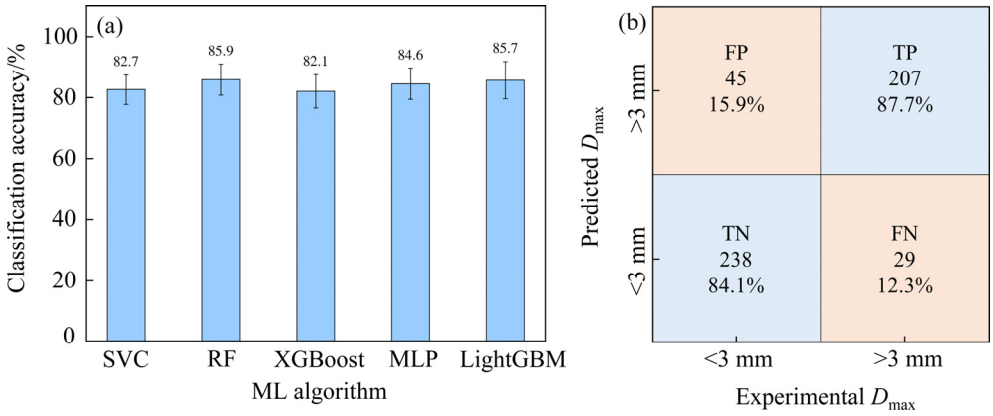

Fig. 6 GFA binary classification: (a) Cross-validation; (b) Confusion matrix of RF

the highest classification accuracy of 85.9%. In detail, one cross-validated classification results of RF were expressed as a confusion matrix in Fig. 6(b), where FP is false positive, TP is true positive, TN is true negative, FN is false negative. For example, 87.7% at upper right corner square, TP, in Fig. 6(b) means that 207 out of 236 positive samples were correctly classified by the trained RF classification model. The prediction accuracy was calculated by 100×(TN+TP)/(TN+TP+FN+FP), which is the ratio of all correctly classified samples. The accuracy for the confusion matrix in Fig. 6(b) was calculated to be 85.7%, which is consistent with (85.9±5.0)% shown in Fig. 6(a). ML models showed good classification accuracy, which could guide the discovery of new soft magnetic MGs.

4 Conclusions

(1) Based on two datasets and a general feature space, ML models can be trained to predict GFA (D_{max}) and magnetic property (B_s) of soft magnetic MGs.

(2) Among five ML algorithms, XGBoost showed the best predictive performance for both D_{max} and B_s prediction.

(3) Knowledge-based feature design can greatly reduce the number of features without significant accuracy loss.

(4) With limited dataset quality, treating D_{max} prediction as a classification problem was more practical than a regression problem.

(5) The predictive accuracy of the trained ML models for properties prediction of soft magnetic MGs was much higher than that of traditional estimation methods based on physical principles.

Acknowledgments

This work was financially supported by the National Key R&D Program of China (No. 022YFB4703400), and the Fundamental Research Funds for the Central Universities, China.

References

[1] WANG W H, DONG C, SHEK C H. Bulk metallic glasses [J]. Materials Science and Engineering R: Reports, 2004, 44(2): 45−89.

[2] HATTA S, EGAMI T, GRAHAM C D Jr. Fe−B−C amorphous alloys with room-temperature saturation induction over 17.5 kG [J]. Applied Physics Letters, 1979, 34(1): 113−115.

[3] HAN Y, DING J, KONG F L, INOUE A, ZHU S L, WANG Z, SHALAAN E, AL-MARZOUKI F. FeCo-based soft magnetic alloys with high Bs approaching 1.75 T and good bending ductility [J]. Journal of Alloys and Compounds, 2017, 691: 364−368.

[4] WANG F, INOUE A, HAN Y, ZHU S L, KONG F L, ZANAEVA E, LIU G D, SHALAAN E, AL-MARZOUKI F, OBAID A. Soft magnetic Fe−Co-based amorphous alloys with extremely high saturation magnetization exceeding 1.9 T and low coercivity of 2 A/m [J]. Journal of Alloys and Compounds, 2017, 723: 376−384.

[5] MAKINO A, KUBOTA T, CHANG C, MAKABE M, INOUE A. FeSiBP bulk metallic glasses with high magnetization and excellent magnetic softness [J]. Journal of Magnetism and Magnetic Materials, 2008, 320(20): 2499−2503.

[6] GAO J E, LI H X, JIAO Z B, WU Y, CHEN Y H, YU T, LU Z P. Effects of nanocrystal formation on the soft magnetic properties of Fe-based bulk metallic glasses [J]. Applied Physics Letters, 2011, 99(5): 052504.

[7] ZHOU Z Q, HE Q F, LIU X D, WANG Q, LUAN J H, LIU C T, YANG Y. Rational design of chemically complex metallic glasses by hybrid modeling guided machine learning [J]. npj Computational Materials, 2021, 7: 138.

[8] WEI Jing, CHU Xuan, SUN Xiang-yu, XU Kun, DENG Hui-xiong, CHEN Ji-gen, WEI Zhong-ming, LEI Ming.

Machine learning in materials science [J]. InfoMat, 2019, 1(3): 338−358.

[9] AYDIN F, DURGUT R. Estimation of wear performance of AZ91 alloy under dry sliding conditions using machine learning methods [J]. Transactions of Nonferrous Metals Society of China, 2021, 31(1): 125−137.

[10] QUAN Guo-zheng, ZHANG Pu, MA Yao-yao, ZHANG Yu-qing, LU Chao-long, WANG Wei-yong. Characterization of grain growth behaviors by BP-ANN and Sellars models for nickle-base superalloy and their comparisons [J]. Transactions of Nonferrous Metals Society of China, 2020, 30(9): 2435−2448.

[11] LIU Xiao-di, LI Xin, HE Quan-feng, LIANG Dan-dan, ZHOU Zi-qing, MA Jiang, YANG Yong, SHEN Jun. Machine learning-based glass formation prediction in multicomponent alloys [J]. Acta Materialia, 2020, 201: 182−190.

[12] SUN Y T, BAI H Y, LI M Z, WANG W H. Machine learning approach for prediction and understanding of glass-forming ability [J]. The Journal of Physical Chemistry Letters, 2017, 8(14): 3434−3439.

[13] FENG Shuo, FU Hua-dong, ZHOU Hui-yu, WU Yuan, LU Zhao-ping, DONG Hong-biao. A general and transferable deep learning framework for predicting phase formation in materials [J]. npj Computational Materials, 2021, 7: 10.

[14] SAMAVATIAN M, GHOLAMIPOUR R, SAMAVATIAN V. Discovery of novel quaternary bulk metallic glasses using a developed correlation-based neural network approach [J]. Computational Materials Science, 2021, 186: 110025.

[15] XIONG Jie, SHI San-qiang, ZHANG Tong-yi. Machine learning prediction of glass-forming ability in bulk metallic glasses [J]. Computational Materials Science, 2021, 192: 110362.

[16] LU Zhi-chao, CHEN Xin, LIU Xiong-jun, LIN De-ye, WU Yuan, ZHANG Yi-bo, WANG Hui, JIANG Sui-he, LI Hong-xiang, WANG Xian-zhen, LU Zhao-ping. Interpretable machine-learning strategy for soft-magnetic property and thermal stability in Fe-based metallic glasses [J]. npj Computational Materials, 2020, 6: 187.

[17] WANG Yu-hao, TIAN Ye-fan, KIRK T, LARIS O, ROSS J H, NOEBE R D, KEYLIN V, ARRÓYAVE R. Accelerated design of Fe-based soft magnetic materials using machine learning and stochastic optimization [J]. Acta Materialia, 2020, 194: 144–155.

[18] LI Xin, SHAN Guang-cun, SHEK C H. Machine learning prediction of magnetic properties of Fe-based metallic glasses considering glass forming ability [J]. Journal of Materials Science & Technology, 2022, 103: 113–120.

[19] YUE Shi-qiang, LIU Tao, KONG Feng-yu, HE Ai-na, ZHANG Hua, ZHANG Tian-long, WANG An-ding, NI Hong-wei, LIU C T. Development of high Bs FeNiBSiNb bulk metallic glasses by using combined CALPHAD and experimental approaches [J]. Journal of Non-Crystalline Solids, 2020, 543: 120108.

[20] FAN Xing-du, JIANG Mu-feng, ZHANG Tao, HOU Long, WANG Chao-xiang, SHEN Bao-long. Thermal, structural and soft magnetic properties of FeSiBPCCu alloys [J]. Journal of Non-Crystalline Solids, 2020, 533: 119941.

[21] HOU Long, YANG Wei-ming, LUO Qiang, FAN Xing-du, LIU Hai-shun, SHEN Bao-long. High Bs of FePBCCu nanocrystalline alloys with excellent soft-magnetic properties [J]. Journal of Non-Crystalline Solids, 2020, 530: 119800.

[22] CAO C C, WANG Y G, ZHU L, MENG Y, ZHAI X B, DAI Y D, CHEN J K, PAN F M. Local structure, nucleation sites and crystallization behavior and their effects on magnetic properties of $Fe_{81}Si_xB_{10}P_{8-x}Cu_1$ (x=0−8) [J]. Scientific Reports, 2018, 8(1): 1243.

[23] TORRENS-SERRA J, BRUNA P, RODRIGUEZ-VIEJO J, ROTH S, CLAVAGUERA-MORA M T. Effect of minor additions on the glass forming ability and magnetic properties of Fe–Nb–B based metallic glasses [J]. Intermetallics, 2010, 18(5): 773−780.

[24] MASTROPIETRO D G, MOYA J A. Design of Fe-based bulk metallic glasses for maximum amorphous diameter (D_{max}) using machine learning models [J]. Computational Materials Science, 2021, 188: 110230.

[25] WANG Wei-hua. Roles of minor additions in formation and properties of bulk metallic glasses [J]. Progress in Materials Science, 2007, 52(4): 540−596.

[26] FANG Shou-shi, XIAO Xue-shan, XIA Lei, LI Wei-huo, DONG Yuan-da. Relationship between the widths of supercooled liquid regions and bond parameters of Mg-based bulk metallic glasses [J]. Journal of Non-Crystalline Solids, 2003, 321(1): 120−125.

[27] WANG Wei-hua. The elastic properties, elastic models and elastic perspectives of metallic glasses [J]. Progress in Materials Science, 2012, 57(3): 487−656.

[28] GUO Sheng, LIU C T. Phase stability in high entropy alloys: Formation of solid-solution phase or amorphous phase [J]. Progress in Natural Science: Materials International, 2011, 21(6): 433−446.

[29] YEH J W, CHEN S K, LIN S J, GAN J Y, CHIN T S, SHUN T T, TSAU C H, CHANG S Y. Nanostructured high-entropy alloys with multiple principal elements: Novel alloy design concepts and outcomes [J]. Advanced Engineering Materials, 2004, 6(5): 299−303.

[30] TAKEUCHI A, INOUE A. Classification of bulk metallic glasses by atomic size difference, heat of mixing and period of constituent elements and its application to characterization of the main alloying element [J]. Materials Transactions, 2005, 46(12): 2817–2829.

[31] MICHAELSON H B. The work function of the elements and its periodicity [J]. Journal of Applied Physics, 1977, 48(11): 4729−4733.

[32] KHOSHGOFTAAR T, DITTMAN D, WALD R, FAZELPOUR A. First order statistics based feature selection: A diverse and powerful family of feature selection techniques [C]//The 11th International Conference on Machine Learning and Applications. Boca Raton: IEEE, 2012: 151−157.

[33] KE Guo-lin, MENG Qi, FINLEY T, WANG Tai-feng, CHEN Wei, MA Wei-dong, YE Qi-wei, LIU T Y. LightGBM: A highly efficient gradient boosting decision tree [C]//Proceedings of the 31st International Conference on Neural Information Processing Systems. Red Hook: Curran Associates Inc., 2017: 3149–3157.

[34] GUYON I, WESTON J, BARNHILL S, VAPNIK V. Gene selection for cancer classification using support vector machines [J]. Machine Learning, 2002, 46(1): 389−422.
[35] HUANG B, YANG Y, WANG A D, WANG Q, LIU C T. Saturated magnetization and glass forming ability of soft magnetic Fe-based metallic glasses [J]. Intermetallics, 2017, 84: 74−81.
[36] KAKEHASHI Y. Modern theory of magnetism in metals and alloys [M]. Springer Science & Business Media, 2013.
[37] MURPHY K P. Machine learning: A probabilistic perspective [M]. 2nd ed. Cambridge, MA: The MIT Press, 2012.
[38] BREIMAN L. Random forests [J]. Machine Learning, 2001, 45(1): 5−32.
[39] CHEN Tian-qi, GUESTRIN C. XGBoost: A scalable tree boosting system [C]//Proceedings of the 22nd ACM SIGKDD International Conference on Knowledge Discovery and Data Mining. New York: Association for Computing Machinery, 2016: 785−794.
[40] BROWNLEE J. Statistical methods for machine learning: Discover how to transform data into knowledge with python [M]. Machine Learning Mastery, 2018.
[41] XIONG Jie, SHI San-qiang, ZHANG Tong-yi. A machine-learning approach to predicting and understanding the properties of amorphous metallic alloys [J]. Materials & Design, 2020, 187: 108378.

基于领域知识辅助的机器学习方法对软磁金属玻璃性能的预测

李 鑫[1,2]，单光存[1,2]，赵鸿滨[3]，石燦鸿[2]

1. 北京航空航天大学 仪器科学与光电工程学院，北京 100191；
2. 香港城市大学 材料科学与工程系，香港特别行政区；
3. 有研科技集团有限公司 智能传感功能材料国家重点实验室，北京 100088

摘 要：提出一种领域知识辅助的机器学习方法，实现对软磁金属玻璃饱和磁化强度(B_s)和临界尺寸(D_{max})的预测。基于公开的实验数据，建立软磁合金数据库。提出一个通用的特征空间，适用于面向不同预测任务的机器学习模型训练。结果表明，机器学习模型的预测能力比基于物理知识的估计方法精度更高。此外，领域知识辅助的特征选择可在有效减少特征数量的同时，不显著降低模型的预测精度。最后，对软磁金属玻璃临界尺寸的二分类预测进行讨论。

关键词：金属玻璃；软磁性；玻璃形成能力；机器学习；材料描述符

(Edited by Bing YANG)